Li, X.; Haramus, V.M.; Li, N.; Gong, Y.; Zhe, Z.; Tian, Z.; Zou, A.:

Preparation and characterization of a pH-responsive mesoporous silica nanoparticle dual-modified with biopolymers

In: Colloids and Surfaces A 548 (2018) 61 - 69
First published online by Elsevier: March 21, 2018

DOI: 10.1016/j.colsurfa.2018.03.047
https://dx.doi.org/10.1016/j.colsurfa.2018.03.047

Preparation and characterization of a pH-responsive mesoporous silica nanoparticle dual-modified with biopolymers

Xiaoran Li[a], Vasil M. Garamus[b], Na Li[c], Yabin Gong[d], Zhe Zhe[e], Zhenfen Tian[a], Aihua Zou[a,*]

[a]Shanghai Key Laboratory of Functional Materials Chemistry, State Key Laboratory of Bioreactor Engineering, East China University of Science and Technology, Shanghai 200237, P.R. China

[b]Helmholtz-Zentrum Geesthacht: Centre for Materials and Coast Research, Institute of Materials Research, Max-Planck-Str. 1, D-21502 Geesthacht, Germany

[c]National Center for Protein Science Shanghai and Shanghai Institute of Biochemistry and Cell Biology, Shanghai 200237, P. R. China

[d]Yueyang Hospital of Integrated Traditional Chinese and Western Medicine, Shanghai University of Traditional Chinese Medicine, Shanghai, 200237, P.R. China

[e]Shanghai Municipal Hospital of Traditional Chinese Medicine, Shanghai University of Traditional Chinese Medicine, Shanghai, 200237, P.R. China

* Corresponding author: Tel.: +86-21-64252231; Fax: +86 -21 -64252231.

E-mail address: aihuazou@ecust.edu.cn

Postal address: East China University of Science and Technology, Shanghai 200237, P.R. China

ABSTRACT

This study was aimed at preparing a long-circulating, highly dispersed and pH-sensitive mesoporous silica nanoparticles (MSNs) carrier via surface modification with polydopamine (PDA) and polyethylene glycol (PEG) i.e. MSNs@PDA-PEG nanoparticles. Small angle X-ray scattering (SAXS) and transmission electron microscopy (TEM) measurements suggested that the MSNs (type MCM-41) of hexagonal structure with the layer of PDA and PEG of thickness ~ 20 nm were successfully prepared. Bovine serum protein (BSA) adsorption experiments showed that less protein was absorbed to MSNs@PDA-PEG nanoparticles after the anchoring of PEG, which confirmed the stealth properties of prepared carriers. Doxorubicin hydrochloride (DOX) was used as model drugs to be encapsulated into MSNs@PDA-PEG nanoparticles (DOX/MSNs@PDA-PEG nanoparticles). DOX/MSNs@PDA-PEG nanoparticles had relatively high entrapment efficiency and drug loading up to 94.2% and 31.4%, respectively. The *in vitro* release profile of DOX/MSNs@PDA-PEG nanoparticles exhibited pH-responsive and gradual drug release. Cytotoxicity assay showed that DOX/MSNs@PDA-PEG nanoparticles had comparable cytotoxicity to A549 cells compared to pure DOX. The intracellular distribution of DOX/MSNs@PDA-PEG nanoparticles was displayed by using confocal laser scanning microscope. It points that PDA and PEG can play "gatekeeper" and stealth roles for MSNs as promising nanocarrier for cancer treatment.

Keywords: MSNs; PEG; PDA; Long-circulating; Highly dispersed; SAXS.

1. Introduction

In recent years, mesoporous silica nanoparticles (MSNs) has attracted great attention due to simple synthesis, tunable pore size and volume, high surface areas, easy functionalization and excellent biocompatibility [1-3]. To date, a series of stimuli-responsive drug delivery systems based on MSNs have been reported [4, 5]. The drug release can be triggered by exogenous or endogenous environment, such as pH [6-9], temperature [10, 11], light [12], enzyme [13], redox potential [12, 14, 15]. A paramount importance step to construct the stimuli-responsive controlled drug release system, using removable "gatekeeper" to cap the pores of MSNs and the cap can be removed via trigger under specific stimulation. Stimuli-responsive gatekeeper materials can be nanoparticles [16], stimuli-sensitive polymers [17, 18], supramolecular assemblies [19]. Xu et al. have developed a dual-receptor targeted delivery system based on mesoporous silica nanoparticles modified with hyaluronic acid (HA) and RGD peptide. MSNs/NH_2-HA-RGD nanoparticles exhibited pH-sensitive drug controlled release behavior [20]. Zhang et al. reported redox-responsive nanogated MSNs by grafting β-CD or adamantane onto the nanopores of MSNs through disulfide [21]. Liu et al. reported phenylboronic acid-conjugated human serum albumin capped MSNs for enzyme-responsive drug delivery [22]. In spite of these polymer-modified MSNs demonstrate good target effect on drug delivery; it is still a challenge to without complicated organic synthesis process. In our study, pH-responsive MSNs modified with polydopamine (PDA) were developed by self-polymerization of dopamine on the surface of MSNs.

PDA, a kind of biomimetic polymer [23], can form a thin and strong sticky layer on the surface of all kinds of organic or inorganic materials [24]. It has been widely used as polymer coating for various biomedical applications including biomineralization [25], biosensor [26, 27], drug delivery [28] and tissue engineering [23, 29], which demonstrates that PDA coater has excellent biocompatibility. Zheng et al. reported that PDA anchored on the surfaces of MSNs (MSNs@PDA) to form a pH-sensitive nanocarrier [30]. However, the strong adsorption of PDA to protein is a severe defect when it is used as drug carrier material [31, 32]. Gu et al. reported the protein adsorption to outer surface of drug carrier system will be identified as a foreign invader by the reticuloendothelial system (RES) or mononuclear phagocyte system (MPS) [33], which would lead to the rapid clearance of MSNs@PDA nanoparticles during the circulation. Polyethylene glycol (PEG) has good water solubility and highly hydrophilicity due to the hydrogen bonds formed with water molecules [34]. In addition, the high fluidity of molecular chain and the large steric repulsion enable them to resist the adsorption of protein in the large extent [3, 35]. Up to now, PEG grafting on the surface of liposome to prolong the circulation time has been widely used

[36-38]. Considering the advantages of both PDA and PEG, the mesoporous silica nanoparticles (MSNs) carrier was modified with polydopamine (PDA) and polyethylene glycol (PEG) in this study (MSNs@PDA-PEG).

Recently pH sensitive release in the DOX/MSNs@PDA-PEG system has been shown [39]. Cell cultures and animal experiments demonstrated that DOX/MSNs@PDA-PEG had improved anticancer efficacy compared to free DOX. DOX/MSNs@PDA-PEG caused a stronger pro-death autophagy compared to free DOX via inhibition of the AKT-mTOR-p70S6K signaling pathway. All those results suggested that the nanocarrier MSNs@PDA-PEG represented a promising effect for breast cancer treatment. However, the achieved drug loading was quite moderate (~ 16%) and the microstructure changes of complexes before and after polymers modification have not been well determined. It was only suggested that the polymer layer was found on the periphery of MSNs by TEM measurements. It is well known that the sustained drug release and the improved anticancer effect of DOX/MSNs@PDA-PEG are highly related with the microstructure of MSNs@PDA-PEG.

In present contribution, we tried to increase drug loading and paid more attention to the structure variation of MSNs after modified with polymers. Small angle X-ray scattering (SAXS), dynamic light scattering (DLS), transmission electron microscopy (TEM) and NMR techniques were employed to characterize the microstructure and the aggregation state of nanocarriers and even obtain the thickness of polymer layer. The effects of PEG on the protein adsorption of bovine serum albumin (BSA) were investigated. DOX was used as model drug to evaluate the drug loading and releasing properties of DOX/MSNs@PDA-PEG nanoparticles. MSNs@PDA-PEG nanoparticles were biologically evaluated with the human lung cancer cell line A549.

2. Materials and methods

2.1 Materials

Tetraethylorthosilicate (TEOS, 98%, Lingfeng Chemical Reagent Co., Ltd., China); Hexadecyl trimethyl ammonium bromide (CTAB, 98%, Sigma-Aldrich, MO, USA); NaOH (Aladdin Chemical Reagent Co., Ltd., China); Doxorubicin hydrochloride (DOX, > 99%, Beijing Huafeng Alliance Bernstein Co., Ltd., China); Dopamine hydrochloride (98%, Adamas Reagent Co., Ltd., China); mPEG-NH_2 (Mw=2000, Aladdin Chemical Reagent Co., Ltd., China); Cell Counting Kit (CCK-8, Dojindo Laboratories, Japan); 4',6-diamidino-2-phenylindole (DAPI, Boster Biological Technology Co., Ltd., USA); All other chemicals are analytical grade or better.

2.2 Synthesis of MSNs

MSNs were synthesized according to the method reported by Lin et al. [40] with a slight modification. CTAB (1.0 g, 2.78 mmol) and NaOH (0.28 g, 7 mmol) were dissolved in 480 mL of water and heated up to 80 ºC. TEOS (5 mL, 4.67 g) was added dropwise into the above solution under vigorous stirring, kept the mixture solution at 80 ºC for 2 h to obtain white precipitate. After the mixture was cool down to room temperature, the white solid product were filtered from the solution and washed with distilled water and ethanol. The solid SiO_2 spheres were dried at 40 ºC under vacuum overnight. To remove the surfactant template (CTAB), the product was heated to 550 ºC at a rising rate of 5 ºC·min^{-1} and calcined for 6 h [41].

2.3 Drug loading and polymer coating

Firstly, a certain amount of MSNs was added to the PBS buffer solution (pH 7.4) containing DOX (40 mL, 0.5 mg·mL^{-1}) and stirred in the dark for 24 h. Secondly, the DOX-loaded MSNs (DOX/MSNs) was collected by centrifugation and washed several times with water.

In order to coat PDA on the surface of DOX/MSNs, 50 mg DOX/MSNs was dispersed in 25 mL Tris-HCl buffer (pH 8.5, 10 mM) and then added 50 mg dopamine hydrochloride to the solution. After the mixture was stirred for 24 h in dark, the PDA-coated DOX/MSNs (DOX/MSNs@PDA) were centrifuged and washed with water to remove the unpolymerized dopamine [42]. MSNs@PDA was also prepared in the same procedure. DOX/MSNs@PDA-PEG nanoparticles were prepared by simply mixed DOX/MSNs@PDA nanoparticles with mPEG-NH_2 at a mass ratio of 1:2 in 25mL Tris-HCl buffer (pH 8.5, 10 mM). The product was purified by centrifugation and washed with water for several times after stirred in the dark for 24 h. All of the above supernatants were collected as the remaining DOX solution. The entrapment efficiency and drug loading was determined by UV-Vis spectrophotometry at 223 nm.

2.4 In vitro drug release studies

The DOX release behavior from nanoparticles was evaluated using the dialysis method [43]. Briefly, 5mg DOX/MSNs@PDA-PEG nanoparticles was dispersed in 5 mL PBS buffer (PBS at different pH values 7.4, 5.0 and 4.0). Then the dispersion was transferred into dialysis bags (MWCO = 8-14KDa) and the bags were placed in jars containing 100 mL PBS buffer. The Jars were gently shaken in a thermostatic shaker bath at 37 ºC. Subsequently, 3 mL released solution was took out at appropriate intervals and replaced by 3mL fresh medium. The DOX/MSNs release experiments were also conducted by the same procedure.

2.5 Characterization

In order to obtain the morphology of MSNs, transmission electron microscopy (TEM) images were

taken by using a JEM-2100 transmission electron microscope (JEOL, Japan). The hydrodynamic diameters (D_h) and zeta potentials were measured by dynamic light scattering (DLS) using DelsaTM Nano C Particle Analyzer (Beckman Coulter, USA). N_2 adsorption/desorption isotherms were measured by an ASAP-2020 accelerated surface area and porosimetry system (Micromeritics, USA). The NMR analysis was determined by AVANCE III 500 NMR spectrometer (BRUKER, Germany). Small-angle X-ray scattering (SAXS) experiments were performed on the BL19U2 beamline of the National Center for Protein Science Shanghai at Shanghai Synchrotron Radiation Facility [44].

2.6 Dispersibility and stability of MSNs@PDA-PEG nanoparticles

5 mg MSNs@PDA and MSNs@PDA-PEG nanoparticles were dispersed in 0.5 mL PBS (pH 7.4) and cell culture medium respectively by sonication for about 30 min. After six hours, the photographs were taken to evaluate the dispersibility and stability of MSNs@PDA and MSNs@PDA-PEG nanoparticles.

2.7 BSA adsorption measurement

The protein adsorption measurement was carried out according to the published method [3]. Briefly, 10 mg MSNs@PDA and MSNs@PDA-PEG nanoparticles were dispersed in 5 mL phosphate buffered saline (PBS) respectively, and then 5 mL BSA solution (1mg·mL^{-1}) was added. The mixture was gently shaken in a thermostatic shaker bath at 37 ºC. After 3 h, the mixture was centrifugalized and upper clear solution was collected. The concentrations of residual BSA were determined by using UV-spectrophotometer at 595 nm. The adsorption of BSA on the surface of MSNs@PDA and MSNs@PDA-PEG nanoparticles were calculated by the following equation:

$q = (C_0 - C_1)\ V/m$, where C_0 and C_1 is the initial BSA and final BSA concentrations in solutions, respectively; V is the total solution volume; m is the weight of nanoparticles added into the solution.

2.8 Cell culture and in vitro cytotoxicity test

The human lung carcinoma cell line A549 was purchased from the American Type Culture Collection (ATCC CCL-185, Manassas, VA, USA). All cells were cultured in the Ham's F12K (Gibco, USA), supplemented with 10% (v/v) fetal bovine serum and antibiotics (100 U·mL^{-1} penicillin and 100 g·mL^{-1} streptomycin) at 37 ºC in a humidified 5% CO_2 atmosphere.

The cytotoxic activities of pure DOX, DOX/MSNs@PDA-PEG and blank MSNs@PDA-PEG nanoparticles towards A549 cells were evaluated by CCK-8 assay. In brief, A549 cells were seeded into 96-well plates at a density of 5 × 10^3 cells/well. After incubated in 100 μL of cell culture medium for 24 h, cells were treated with the pure DOX, DOX/MSNs@PDA-PEG nanoparticles suspension (the

concentrations of DOX was 0.3, 0.6, 1.3, 2.5 and 5.0μg·mL^{-1}) and the MSNs@PDA-PEG nanoparticles suspension (the same volume as that used for DOX/MSNs@PDA-PEG nanoparticles suspension). 10 μL CCK-8 was added to each well after cells were cultured for 24 h or 48 h and then plates were incubated for 1 h at 37 ºC. Finally, the absorbance was measured at 450 nm using microplate reader.

2.9 Cell uptake

Confocal fluorescence microscopy was used to observe the cells uptake and the intracellular distribution of pure DOX and DOX/MSNs@PDA-PEG nanoparticles suspension in A549 cells. In brief, A549 cells were seeded into 6-well plates with 14mm^2 sterile glass coverslips and cultured in 2 mL of cell culture medium for 24 h. The medium was replaced by DOX/MSNs@PDA-PEG nanoparticles suspension, the concentration of DOX was 20 μg·mL^{-1}. Three hours later, the cells were fixed by 4% paraformaldehyde for 20 min, and then stained with 4, 6-diamidino-2-phenylindole (DAPI) for 30 min. The cells were imaged by confocal fluorescence microscopy.

3. Results and Discussion

3.1 Synthesis and characterization of nanoparticles

The prepared process of MSNs@PDA-PEG nanoparticles with PDA as gatekeeper and PEG as dispersibility-enhancer was shown in the Scheme 1. MSNs were synthesized by dropping TEOS to the mixture solution of CTAB and NaOH, then the surfactant CTAB was removed by calcination [40]. The morphology of MSNs was verified by TEM. As shown in Fig. 1A, MSNs are nearly smooth spherical shape and many pores are clearly visible. The average diameter of MSNs was about 100 nm, which was similar to the result of DLS (115.5 ± 0.05 nm, Table S1). The pore volume (V_t), pore size distribution (D_p) and specific surface area (S_{BET}) were determined by N_2 adsorption-desorption analysis (Fig. 1C). The adsorption isotherm of MSNs exhibited a type IV isotherm according to IUPAC classification, which was characteristic of mesoporous materials with high surface area and narrow pore size distribution [45]. As shown in Fig. 1C, the Nitrogen adsorption slowly increased at low pressure area and the pore filling form from monolayer to multilayer formation could be observed. At $P/P_o \approx 1$, it appeared hysteresis phenomenon, which assign to the H_3 type. The BET surface area (S_{BET}) and the pore volume (V_t) were about 490.74 m^2·g^{-1} and 0.37cm^3·g^{-1}, respectively. The pore size distribution (D_p) was about 2.34 nm (Fig. 1D). In a word, this kind of material could be used to delivery small molecule drugs.

MSNs@PDA nanoparticles were prepared by coating PDA on the surface of MSNs since dopamine could self-polymerization in the basic condition. As shown in Fig. 1B, the surface of MSNs@PDA

nanoparticles was much rougher than MSNs and a block layer (~ 5 nm) can be seen clearly on the surface of MSNs after the modification of PDA. The hydrodynamic diameter (D_h) of MSNs@PDA nanoparticles (123.6 ± 0.08 nm, Table S1) was slightly larger than MSNs (115.5 ± 0.05 nm), which indicated the presence of PDA. The estimated thickness of electrical double layer (inverse Debye-Hückel length) is in order of XX nm.

MSNs@PDA-PEG nanoparticles were prepared by further modified MSNs@PDA nanoparticles with PEG since PDA possesses plentiful chemically-active catechol and quinone groups [46]. The D_h of MSNs@PDA-PEG nanoparticles (163.2 ± 0.10 nm, Table S1) was much larger than MSNs@PDA nanoparticles, which can be attributed to the existence of hydration layer from PEG chains [47]. ^{1}H NMR spectra of nanoparticles was measured, a singlet at δ = 3.63 ppm emerged in the MSNs@PDA-PEG nanoparticles compared with MSNs@PDA nanoparticles (Fig. 2), which indicated the presence of PEG [48]. In addition, the FTIR spectra of samples were also proved that PEG was successfully grafted on MSNs@PDA-PEG nanoparticles (Fig. S1).

3.2 SAXS *analysis*

In this study, the small-angle x-ray scattering (SAXS) technique was employed to characterize the microstructure and the aggregation state of MSNs, MSNs@PDA, MSNs@PDA-PEG and MSNs/DOX@PDA-PEG, which is an important parameter to study the structural property of nanoparticles. As shown in Fig. 3A, three Bragg peaks of MSNs were clearly visible at the q values of 1.56, 2.73, 3.56 nm^{-1}. The ratio of their spacings was 1, $1/\sqrt{3}$, $1/\sqrt{4}$, which can be assigned to the 2D hexagonal lattice of mesoporous [49]. In the case of polymer-modified MSNs, although the position of peaks has changed, the spacing ratio was still the same as MSNs, which indicated that the symmetry of structure did not change. Interestingly, there was only one peak after DOX loaded into the MSNs@PDA-PEG nanoparticles, it means that the amount of empty pore was significantly reduced after DOX loading and there was no long range order of empty pores. From the position of 1st peaks, the lattice constant a of pure MSNs and modified MSNs was determined according to the equation of $a = 4\pi/\sqrt{3} * q$. MSNs, the polymer-modified MSNs and the drug-loaded MSNs appeared peak at q = 1.56, q = 1.63 and q = 1.63 nm^{-1} leading to the lattice constants a of 4.65 4.45 and 4.45 nm, respectively. The observed small decreasing in the lattice parameter value can be explained by the non-homogeneous distribution of pores in the MSNs. The outer pore has a higher lattice parameter, when polymer or drug adsorption part of it would lead to the decrease of lattice parameter. In the same time, polymer or drug adsorption also

leads to the decreasing of scattering volume of pores (decreasing intensity of Bragg peaks). It looks that pores in the center of MSNs are closed packed than in surface region may be due to some distortions at the periphery of MSNs.

The linearity of the ln-ln scattering profile revealed the fractals property of the formed nanoparticles. As shown in Fig. 3B, all samples were mass fractals (D_m) at $q < 0.14$ nm^{-1} and surface fractals (D_s) at $q > 0.14$ nm^{-1}. It means that structure changes volume to surface properties at lengths of about 10 nm ($\sim 1/q$). This implied that the growth and the aggregation of samples might be a kind of nonlinear process. The variation of fractal dimension was shown in the Table 1, it can be seen that the value D_m decreased from -1.81 to -1.68 after grafting PEG. The phenomenon of decrease indicated that the structure of MSNs@PDA-PEG nanoparticles became less compact. In addition, the D_s of MSNs and MSNs@PDA nanoparticles were basically the same (Table 1) and the results indicated the surface of two samples was rough. However, the D_s decreased after the coating of PEG on MSNs@PDA nanoparticles, which demonstrated that the surface of MSNs@PDA-PEG nanoparticles became rougher. As it was reported, PEG could form brush structure on the surface of MSNs@PDA-PEG nanoparticles [50], which increased the steric hindrance between nanoparticles [35]. Thus, PEG coating could increase the dispersion of nanoparticles and MSNs@PDA-PEG nanoparticles was more stable in aqueous solution. This phenomenon will be further discussed in section *3.3*.

3.3 The effect of grafting PEG on the surface of MSNs@PDA nanoparticles

Although MSNs@PDA nanoparticles are a promising stimuli-response drug carrier, the aggregation and the strong protein adsorption on the surface of MSNs@PDA have limited their clinical applications [31, 32]. Here, PEG was chosen to increase the dispersibility and prolong the circulation time of MSNs@PDA nanoparticles as drug delivery system. 5 mg MSNs@PDA and MSNs@PDA-PEG nanoparticles were dispersed in the 0.5 mL PBS (pH 7.4) and cell culture medium to evaluate their dispersibility, respectively. As shown in Fig. 4A, although MSNs@PDA nanoparticles were stable in PBS, it was aggregated after dispersing in the cell culture medium. In contrast, MSNs@PDA-PEG nanoparticles can remain stable in both PBS and cell culture medium. In order to study the stable mechanism of nanoparticles, polydispersity index (PDI) and zeta potential were determined. PDI indicates the width of the particle size distribution and higher value demonstrates sample is easily aggregated [51]. As shown in Table S1, the PDI of MSNs@PDA-PEG nanoparticles (0.11) was much smaller than the MSNs@PDA nanoparticles (0.19), indicating that MSNs@PDA-PEG nanoparticles had

better particle size distribution after the modification of PEG. Surface charge was used to assess the physical stability of system in a medium. The higher absolute value of zeta potential is, the better dispersion and stability of colloidal system is [52]. As shown in Fig. 4B, the zeta potential value of MSNs@PDA and MSNs@PDA-PEG nanoparticles was -13.26 ± 0.12 mV and -28.07 ± 0.07 mV, respectively. The absolute zeta potential value of MSNs@PDA-PEG nanoparticles was improved after grafting PEG compared with that of MSNs@PDA. Therefore, the electrostatic repulsion between the nanoparticles could make MSNs@PDA-PEG more stable definitely.

To further investigate the effectiveness of PEG modification to MSNs@PDA nanoparticles, the BSA adsorption to the surface of MSNs@PDA and MSNs@PDA-PEG nanoparticles was measured according to the report by Zhao et al. [3]. As shown in Fig. 4B, it was found that less BSA was absorbed to the MSNs@PDA-PEG nanoparticles (1.2 ± 0.05 wt%) when compared with that of MSNs@PDA nanoparticles (2.5 ± 0.05 wt%). This phenomenon can be attributed to the large steric repulsion of PEG on the surface of MSNs@PDA-PEG nanoparticles resulted in the less protein adsorption [3, 35]. The above results indicated that the hydrophilic PEG could reduce protein adsorption and increase the stability of nanoparticles, which were beneficial to improve the biocompatibility and prolong the circulation time of MSNs nanoparticles.

3.4 The drug loading and stimuli-responsive drug release in vitro

To investigate the drug loading ability of MSNs@PDA-PEG nanoparticles, the anticancer drug DOX was used as model drug. In the PBS solution (pH 7.4), drugs could be loaded into MSNs through physical absorption and electrostatic interaction between DOX and MSNs. DOX/MSNs@PDA-PEG nanoparticles had relatively high entrapment efficiency and drug loading up to 94.2% and 31.4%, respectively. The drug loading of DOX/MSNs@PDA-PEG nanoparticles was bigger than that of the mesoporous silica nanoparticles modified with hyaluronic acid (19.8%) [53], ethylcellulose (18.8%) [54] and poly(2-(diethylamino)ethyl methacrylate) (13.1%) [47], respectively. The high entrapment efficiency of DOX in the MSNs@PDA-PEG nanoparticles further confirmed the successful coating of PDA and PEG on the surface of MSNs.

The *in vitro* release behavior of DOX from DOX/MSNs and DOX/MSNs@PDA-PEG nanoparticles was studied by using the dialysis method. As shown in the Fig. 5, the cumulative release of DOX from DOX/MSNs after 24 h and 60 h was 65.5% and 85.4%, respectively. However, the drug release profile from MSNs@PDA-PEG nanoparticles was significant different, the cumulative release of DOX after 24 h and 60 h was 26.1 % and 35.5 %, respectively. Obviously, the release rate of DOX from the

DOX/MSNs@PDA-PEG nanoparticles was slower compared with the DOX/MSNs at neutral condition. As shown in the SAXS experiments, PDA was successfully modified on the surface of MSNs, with 7.6 nm thickness. Therefore, it was expected that PDA coating as the gatekeeper would reduce the release rate of DOX/MSNs in pH 7.4 conditions. For the DOX/MSNs@PDA-PEG nanoparticles, the DOX release rate could be tuned by the pH values of release medium. As shown in Fig. 5B, the DOX release rate was clearly increased with the decrease of pH values (at pH of 5.0 and 4.0). Similar phenomenon was observed by Chang [55], and it was explained that PDA could detach from the surface of MSNs in the acidic condition, and lead to the faster drug release. According to the above physical chemical properties determined for MSNs@PDA-PEG nanoparticles, PEG grafted on the surface of MSNs@PDA nanoparticles would enhance the blood circulation half-life of MSNs@PDA-PEG nanoparticles through hindering the carrier-macrophage interactions directly [38]. This long-circulating property increased the selective accumulation of MSNs@PDA-PEG nanoparticles at tumor sites, while PDA was expected to be sensitive to the acidic environment inside the endosomes and lysosomes of tumor cells [56]. So PDA and PEG dual-modified MSNs can be used as potential drug carrier.

3.5 Biological evaluation in cell cultures experiments

The cell uptake and intracellular distribution of DOX/MSNs@PDA-PEG nanoparticles play a significant role in their application as drug carrier. In this study, the cell uptake and intracellular distribution of DOX/MSNs@PDA-PEG nanoparticles by A549 cells were determined by using confocal microscopy with differential interference contrast channel, where the blue channel was for DAPI and the red channel was for DOX. Briefly, cells were imaged when incubated with the pure DOX or the DOX/MSNs@PDA-PEG nanoparticles suspension (at equivalent DOX concentration of 5μg·mL^{-1}) for 3 h. As illustrated in Fig. 6(A1), free DOX was mainly located in the nuclei after cells were incubated with pure DOX for 3 h. However, the red fluorescence was found both in the cell nucleus and the cytoplasm when cultivated A549 cells with DOX/MSNs@PDA-PEG nanoparticles for 3 h (Fig. 6(A2)). This phenomenon implied that DOX/MSNs@PDA-PEG nanoparticles could enter cells, and then DOX molecules slowly released from DOX/MSNs@PDA-PEG nanoparticles and eventually came into the nucleus of cancer cells. This process should be different with pure DOX, and so does the intracellular distribution of DOX/MSNs@PDA-PEG nanoparticles.

Fig. 6B presented the cytotoxicity of the investigated samples (free DOX, DOX/MSNs@PDA-PEG and MSNs@PDA-PEG nanoparticles) with the human lung carcinoma cell line A549. As shown in Fig. 6B, MSNs@PDA-PEG nanoparticles had no obvious cytotoxicity towards A549 cells at all

concentrations, indicating that it had good biocompatibility. The effects of free DOX and DOX/MSNs@PDA-PEG nanoparticles depended on the drug concentration and the incubation time. The cytotoxicity of free DOX and DOX/MSNs@PDA-PEG nanoparticles increased with the increase of their concentration. The cytotoxicity of DOX/MSNs@PDA-PEG nanoparticles was slightly lower than that of the pure DOX after 24 h incubation, while the cytotoxicity of DOX/MSNs@PDA-PEG nanoparticles was higher than that free DOX after 48 h incubation (Fig. 6(B2)). This result could be attributed to the controlled release of DOX from DOX/MSNs@PDA-PEG nanoparticles as suggested by the *in vitro* drug release experiments. Moreover, the cell uptake and intracellular distribution of DOX/MSNs@PDA-PEG nanoparticles could also imply that the DOX would take more time to come into the nuclei of cancer cells. By all these results, it can be expected that the long-circulating and pH-sensitive MSNs@PDA-PEG nanoparticle can be used as potential drug carrier for treating tumor.

The half inhibition concentrations (IC_{50}) of pure DOX and DOX/MSNs@PDA-PEG nanoparticles for 48 h were 0.60 ± 0.14 $\mu g \cdot mL^{-1}$ and 0.78 ± 0.32 $\mu g \cdot mL^{-1}$, respectively. The IC_{50} values of pure DOX and DOX/MSNs@PDA-PEG nanoparticles suggested that both had comparable performance of DOX against A549 cells, while the cytotoxicity of DOX/MSNs@PDA-PEG nanoparticles was lower than that free DOX after 48 h incubation. This could be explained from the results of *in vitro* release measurements and cell uptake assay. DOX/MSNs@PDA-PEG nanoparticles was supposed to be ingested into the cells by endocytosis; then DOX was released slowly from nanoparticles at cytoplasm and further diffused into cell nuclei, which should be quite different from the behavior of pure DOX. Hence, the performance of DOX/MSNs@PDA-PEG nanoparticles may not be worse than pure DOX for *in vitro* models.

4. Conclusions

In summary, a kind of long-circulating, highly dispersed and pH-sensitive drug delivery system MSNs@PDA-PEG has been developed, where the biodegradable PDA as the gatekeeper and PEG as dispersibility-enhancer were both grafted on the surface of MSNs. NMR technique proved that PEG successfully modified on the surface of PDA. SAXS analysis indicated that MSNs were hexagonal structure and the modified with PEG improved the dispersion of nanoparticles. In addition, it was the first time to determine the thickness of polymer (PDA and PEG) by using the SAXS measurement. BSA adsorption test confirmed that PEG modification reduced protein adsorption and increased the stability of nanoparticles. Furthermore, DOX/MSNs@PDA-PEG nanoparticles exhibited good anti-cancer efficacy for human lung A549 cell through *in vitro* growth inhibition study. To further improve the advantage of

MSNs as efficient drug carrier, targeting molecules will be modified on the surface of MSNs@PDA-PEG nanoparticles by dual-receptor binding for cancer therapy in our future work.

Acknowledgment

This work was supported by the National Natural Science Foundation of China (No. 31200617), Shanghai Natural Science Foundation (No. 15ZR1409900), and Knowledge Innovation Program of CAS (No. 2013KIP103). Thanks to the staff of the BL19U2 beamline at the National Center for Protein Science Shanghai and the Shanghai Synchrotron Radiation Facility for assistance during data collection.

Reference

[1] F. Tang, L. Li, D. Chen, Mesoporous silica nanoparticles: synthesis, biocompatibility and drug delivery, Adv. mater. 24(12) (2012) 1504-34.

[2] K. Möller, T. Bein, Talented Mesoporous Silica Nanoparticles, Chem. Mater. 29(1) (2017) 371-88.

[3] Q. Zhao, C. Wang, Y. Liu, J. Wang, Y. Gao, X. Zhang, T. Jiang, S. Wang, PEGylated mesoporous silica as a redox-responsive drug delivery system for loading thiol-containing drugs, Int. J. Pharm. 477(1-2) (2014) 613-22.

[4] V. Mamaeva, J.M. Rosenholm, L.T. Bate-Eya, L. Bergman, E. Peuhu, A. Duchanoy, L.E. Fortelius, S. Landor, D.M. Toivola, M. Linden, C. Sahlgren, Mesoporous silica nanoparticles as drug delivery systems for targeted inhibition of Notch signaling in cancer, Mol. ther. 19(8) (2011) 1538-46.

[5] G.F. Luo, W.H. Chen, Y. Liu, Q. Lei, R.X. Zhuo, X.Z. Zhang, Multifunctional enveloped mesoporous silica nanoparticles for subcellular co-delivery of drug and therapeutic peptide, Sci. rep. 4 (2014) 6064.

[6] Q. Zheng, Y. Hao, P. Ye, L. Guo, H. Wu, Q. Guo, J. Jiang, F. Fu, G. Chen, A pH-responsive controlled release system using layered double hydroxide (LDH)-capped mesoporous silica nanoparticles, J. Mater. Chem. B 1(11) (2013) 1644.

[7] C. Hu, L. Yu, Z. Zheng, J. Wang, Y. Liu, Y. Jiang, G. Tong, Y. Zhou, X. Wang, Tannin as a gatekeeper of pH-responsive mesoporous silica nanoparticles for drug delivery, RSC Adv. 5(104) (2015) 85436-41.

[8] F. Muhammad, M. Guo, W. Qi, F. Sun, A. Wang, Y. Guo, G. Zhu, pH-Triggered controlled drug release from mesoporous silica nanoparticles via intracelluar dissolution of ZnO nanolids, J. Am. Chem. Soc. 133(23) (2011) 8778-81.

[9] L. Du, H.A. Khatib, J.F. Stoddart, J.I. Zink, Controlled-access hollow mechanized silica nanocontainers, J. Am. Chem. Soc. 131 (2009) 15136-42.

[10] E. Aznar, L. Mondragon, J.V. Ros-Lis, F. Sancenón, M.D. Marcos, Finely tuned temperature-controlled cargo release using paraffin-capped mesoporous silica nanoparticles, Angew. Chem. Int. Ed. 50(47) (2011) 11172-5.

[11] A. Schlossbauer, P. Gramlich, S. Warncke, T. Bein, A programmable DNA-based molecular valve for

colloidal mesoporous silica, Angew. Chem. Int. Ed. 49(28) (2010) 4734-7.

[12] Y. Wang, K. Wang, J. Zhao, X. Liu, J. Bu, X. Yan, R. Huang, Multifunctional mesoporous silica-coated graphene nanosheet used for chemo-photothermal synergistic targeted therapy of glioma, J. Am. Chem. Soc. 135 (2013) 4799-804.

[13] K.J. Schlossbauer, T. Bein, Biotin-avidin as a protease-responsive cap system for controlled guest release from colloidal mesoporous silica, Angew. Chem. Int. Ed. 48(17) (2009) 3092-5.

[14] L. Chen, X. Zhou, W. Nie, Q. Zhang, W. Wang, Y. Zhang, C. He, Multifunctional Redox-Responsive Mesoporous Silica Nanoparticles for Efficient Targeting Drug Delivery and Magnetic Resonance Imaging, ACS appl. mater. interfaces 8(49) (2016) 33829-41.

[15] B.H. Kim, C. Park, H. Lee, H.J. Park, C. Kim, Glutathione-induced intracellular release of guests from mesoporous silica nanocontainers with cyclodextrin gatekeepers, Adv. mater. 22(38) (2010) 4280-3.

[16] S. Giri, B.G. Trewyn, M.P. Stellmaker, V.S.Y. Lin, Stimuli-Responsive Controlled-Release Delivery System Based on Mesoporous Silica Nanorods Capped with Magnetic Nanoparticles, Angew. Chem. Int. Ed. 117(32) (2005) 5166-72.

[17] R. Cheng, F. Meng, C. Deng, H.A. Klok, Z. Zhong, Dual and multi-stimuli responsive polymeric nanoparticles for programmed site-specific drug delivery, Biomaterials 34(14) (2013) 3647-57.

[18] R. Liu, P. Liao, J. Liu, P. Feng, Responsive polymer-coated mesoporous silica as a pH-sensitive nanocarrier for controlled release, Langmuir 27(6) (2011) 3095-9.

[19] L. Du, S. Liao, H.A. Khatib, J.F. Stoddart, J.I. Zink, Controlled-access hollow mechanized silica nanocontainers, J. Am. Chem. Soc. 131(42) (2009) 15136-42.

[20] H. Xu, Z. Wang, Y. Li, Y. Guo, H. Zhou, Y. Li, F. Wu, L. Zhang, X. Yang, B. Lu, Z. Huang, W. Xu, P. Xu, Preparation and characterization of a dual-receptor mesoporous silica nanoparticle–hyaluronic acid–RGD peptide targeting drug delivery system, RSC Adv. 6(46) (2016) 40427-35.

[21] Q. Zhang, F. Liu, K.T. Nguyen, X. Ma, X. Wang, B. Xing, Y. Zhao, Multifunctional Mesoporous Silica Nanoparticles for Cancer-Targeted and Controlled Drug Delivery, Adv. Funct. Mater. 22(24) (2012) 5144-56.

[22] J. Liu, B. Zhang, Z. Luo, X. Ding, J. Li, L. Dai, J. Zhou, X. Zhao, J. Ye, K. Cai, Enzyme responsive mesoporous silica nanoparticles for targeted tumor therapy in vitro and in vivo, Nanoscale 7(8) (2015) 3614-26.

[23] H. Lee, S.M. Dellatore, W.M. Miller, P.B. Messersmith, Mussel-inspired surface chemistry for multifunctional coatings, Science 318(5849) (2007) 426-30.

[24] L. Zhang, S. Roy, Y. Chen, E.K. Chua, K.Y. See, X. Hu, M. Liu, Mussel-inspired polydopamine coated hollow carbon microspheres, a novel versatile filler for fabrication of high performance syntactic foams, ACS appl. mater. interfaces 6(21) (2014) 18644-52.

[25] S. Kim, C.B. Park, Mussel-inspired transformation of CaCO3 to bone minerals, Biomaterials 31(25) (2010) 6628-34.

[26] Y. Fu, P. Li, Q. Xie, X. Xu, L. Lei, C. Chen, C. Zou, W. Deng, S. Yao, One-Pot Preparation of Polymer-Enzyme-Metallic Nanoparticle Composite Films for High-Performance Biosensing of Glucose and Galactose, Adv. Funct. Mater. 19(11) (2009) 1784-91.

[27] F. Li, Y. Feng, L. Yang, L. Li, C. Tang, B. Tang, A selective novel non-enzyme glucose amperometric biosensor based on lectin-sugar binding on thionine modified electrode, Biosens. Bioelectron. 26(5) (2011) 2489-94.

[28] Q. Liu, B. Yu, W. Ye, F. Zhou, Highly selective uptake and release of charged molecules by pH-responsive polydopamine microcapsules, Macromol. biosci. 11(9) (2011) 1227-34.

[29] S.H. Ku, C.B. Park, Human endothelial cell growth on mussel-inspired nanofiber scaffold for vascular tissue engineering, Biomaterials 31(36) (2010) 9431-7.

[30] Q. Zheng, T. Lin, H. Wu, L. Guo, P. Ye, Y. Hao, Q. Guo, J. Jiang, F. Fu, G. Chen, Mussel-inspired polydopamine coated mesoporous silica nanoparticles as pH-sensitive nanocarriers for controlled release, Int. J. Pharm. 463(1) (2014) 22-6.

[31] R. Gao, L. Zhang, Y. Hao, X. Cui, D. Liu, M. Zhang, Y. Tang, Novel polydopamine imprinting layers coated magnetic carbon nanotubes for specific separation of lysozyme from egg white, Talanta. 144 (2015) 1125-32.

[32] Z. Xia, Z. Lin, Y. Xiao, L. Wang, J. Zheng, H. Yang, G. Chen, Facile synthesis of polydopamine-coated molecularly imprinted silica nanoparticles for protein recognition and separation, Biosens. Bioelectron. 47 (2013) 120-6.

[33] J. Gu, S. Su, M. Zhu, Y. Li, W. Zhao, Y. Duan, J. Shi, Targeted doxorubicin delivery to liver cancer cells by PEGylated mesoporous silica nanoparticles with a pH-dependent release profile, J. Microporous Mesoporous Mater. 161 (2012) 160-7.

[34] J. Jiao, X. Li, S. Zhang, J. Liu, D. Di, Y. Zhang, Q. Zhao, S. Wang, Redox and pH dual-responsive PEG and chitosan-conjugated hollow mesoporous silica for controlled drug release, Sci. Eng. C Mater. Biol. Appl. 67 (2016) 26-33.

[35] Q. He, J. Zhang, J. Shi, Z. Zhu, L. Zhang, W. Bu, L. Guo, Y. Chen, The effect of PEGylation of

mesoporous silica nanoparticles on nonspecific binding of serum proteins and cellular responses, Biomaterials 31(6) (2010) 1085-92.

[36] D. Papahadjopoulos, T.M. Allen, A. Gabizon, E. Mayhew, K. Matthay, S.K. Huang, K.D. Lee, M.C. Woodle, D.D. Lasic, C. Redemann, Sterically stabilized liposomes: improvements in pharmacokinetics and antitumor therapeutic efficacy, Proc. Natl. Acad. Sci. USA 88 (1991) 11460-4.

[37] A.S. Abu Lila, K. Nawata, T. Shimizu, T. Ishida, H. Kiwada, Use of polyglycerol (PG), instead of polyethylene glycol (PEG), prevents induction of the accelerated blood clearance phenomenon against long-circulating liposomes upon repeated administration, Int. J. Pharm. 456(1) (2013) 235-42.

[38] V.P. Torchilin, V.G. Omelyanenko, M.I. Papisov, A.A. Bogdanov Jr., V.S. Trubetskoy, J.N. Herron, C.A. Gentry, Poly(ethylene glycol) on the liposome surface: on the mechanism of polymer-coated liposome longevity, Biochim. Biophys. Acta. 1195 (1994) 11-20.

[39] Y.H. Duo, Y. Li, C.K. Chen, B.Y. Liu, X.Y. Wang, X.W. Zeng and H.B. Chen, DOX-loaded pH-sensitive mesoporous silica nanoparticles coated with PDA and PEG induce pro-death autophagy in breast cancer, RSC Adv. 7(63) (2017) 39641-50.

[40] B.G. Trewyn, I.I. Slowing, V.S. Lin, Mesoporous silica nanoparticles for intracellular delivery of membrane-impermeable proteins , J. Am. Chem. Soc. 129 (2007) 8845-9.

[41] M. Muller, B. Kessler, Deposition from dopamine solutions at Ge substrates: an in situ ATR-FTIR study, Langmuir 27(20) (2011) 12499-505.

[42] L. Guo, Q. Liu, G. Li, J. Shi, J. Liu, T. Wang, G. Jiang, A mussel-inspired polydopamine coating as a versatile platform for the in situ synthesis of graphene-based nanocomposites, Nanoscale 4(19) (2012) 5864-7.

[43] D. Chang, Y. Gao, L. Wang, G. Liu, Y. Chen, T. Wang, W. Tao, L. Mei, L. Huang, X. Zeng, Polydopamine-based surface modification of mesoporous silica nanoparticles as pH-sensitive drug delivery vehicles for cancer therapy, J. Colloid Interface Sci. 463 (2016) 279-87.

[44] W.H. Lv, S.N. Zhao, H. Yu, N. Li, V.M. Garamus, Y.Y. Chen, P.H. Yin, R.G. Zhang, Y.B. Gong, A.H. Zou, Brucea javanica oil-loaded nanostructure lipid carriers (BJO NLCs): Preparation, characterization and in vitro evaluation, Colloids Surf. A 504 (2016) 312-9.

[45] X. Zheng, J. Zhang, J. Wang, X. Qi, J.M. Rosenholm, K. Cai, Polydopamine Coatings in Confined Nanopore Space: Toward Improved Retention and Release of Hydrophilic Cargo, J. Phys. Chem. C 119(43) (2015) 24512-21.

[46] X. Wang, J. Zhang, Y. Wang, C. Wang, J. Xiao, Q. Zhang, Y. Cheng, Multi-responsive

photothermal-chemotherapy with drug-loaded melanin-like nanoparticles for synergetic tumor ablation, Biomaterials 81 (2016) 114-24.

[47] T. Chen, W. Wu, H. Xiao, Y. Chen, M. Chen, J. Li, Intelligent Drug Delivery System Based on Mesoporous Silica Nanoparticles Coated with an Ultra-pH-Sensitive Gatekeeper and Poly(ethylene glycol), J. ACS Macro. Lett. 5(1) (2016) 55-8.

[48] H.J. Cho, I.S. Yoon, H.Y. Yoon, H. Koo, Y.J. Jin, S.H. Ko, J.S. Shim, K. Kim, I.C. Kwon, D.D. Kim, Polyethylene glycol-conjugated hyaluronic acid-ceramide self-assembled nanoparticles for targeted delivery of doxorubicin, Biomaterials 33(4) (2012) 1190-200.

[49] K. Brandenburg, W. Richter, M.H. Koch , H.W. Meyer , U. Seydel, Characterization of the nonlamellar cubic and HII structures of lipid A from Salmonella enterica serovar Minnesota by X-ray diffraction and freeze-fracture electron microscopy, Chem. Phys. Lipids 91 (1998) 53-69.

[50] Z.H. Li, Y.H Sun, J. Wang, Y. Liu, B.Z. Dong, Fractals of Silica Aggregates, Beijing Synchrotron Radiation Facility (2) (2001) 32-8.

[51] S. Das, W.K. Ng, R.B. Tan, Are nanostructured lipid carriers (NLCs) better than solid lipid nanoparticles (SLNs): development, characterizations and comparative evaluations of clotrimazole-loaded SLNs and NLCs? Eur. J. pharm. Sci. 47(1) (2012) 139-51.

[52] X. Fan, J. Chen, Q. Shen, Docetaxel-nicotinamide complex-loaded nanostructured lipid carriers for transdermal delivery, Int. J. Pharm. 458(2) (2013) 296-304.

[53] Q.F. Zhao, J. Liu, W.Q. Zhu, C.S. Sun, D.H. Di, Y.Zhang, P. Wang, Z.Y. Wang, S.L. Wang, Dual-stimuli responsive hyaluronic acid-conjugated mesoporous silica for targeted delivery to CD44-overexpressing cancer cells, Acta. Biomater. 23 (2015) 147-56.

[54] Y. C. Hacene, A. Singh, G. V. Mooter, Drug loaded and ethylcellulose coated mesoporous silica for controlled drug release prepared using a pilot scale fluid bed system, Int. J. Pharm. 506 (2016) 138-47.

[55] D. Chang, Y. Gao, L. Wang, G. Liu, Y. Chen, T. Wang, W. Tao, L. Mei, L. Huang, X. Zeng, Polydopamine-based surface modification of mesoporous silica nanoparticles as pH-sensitive drug delivery vehicles for cancer therapy, J. colloid interface Sci. 463 (2016) 279-87.

[56] C. Li, J. Xia, X. Wei, H. Yan, Z. Si, S. Ju, pH-Activated Near-Infrared Fluorescence Nanoprobe Imaging Tumors by Sensing the Acidic Microenvironment, Adv. Funct. Mater.20(14) (2010) 2222-30.

Figure and Table Legends:

Scheme 1 The preparation process of MSNs@PDA-PEG and DOX/MSNs@PDA-PEG nanoparticles.

Fig. 1. TEM image of MSNs (A), TEM image of MSNs@PDA nanoparticles (B); N_2 adsorption/desorption isotherms of MSNs (C); Pore size distribution from BJH adsorption of MSNs (D).

Fig. 2. ^{1}H NMR spectra of MSNs@PDA and MSNs@PDA-PEG nanoparticles.

Fig. 3. SAXS curves of ln I (q) versus q, the structure of samples was determined from the position of peaks (A); Plots of ln I (q) versus ln q, it revealed the fractals property of the formed nanoparticles (B).

Fig. 4. Photos of MSNs@PDA and MSNs@PDA-PEG nanoparticles in different medium (A); The absorbance of BSA to the surface of MSNs@PDA and MSNs@PDA-PEG nanoparticles (B), the zeta potential of MSNs@PDA and MSNs@PDA-PEG nanoparticles (B).

Fig. 5. *In vitro* release profiles of DOX/MSNs nanoparticles (A) and DOX/MSNs@PDA-PEG nanoparticles (B).

Fig. 6. (A) Cellular uptake of pure DOX and DOX/MSNs@PDA-PEG nanoparticles with A549 cells revealed by confocal microscopy images; (B) In vitro cytotoxicity of DOX/MSNs@PDA-PEG nanoparticles against A549 cells after exposed different times: 24 h (B1) and 48 h (B2).

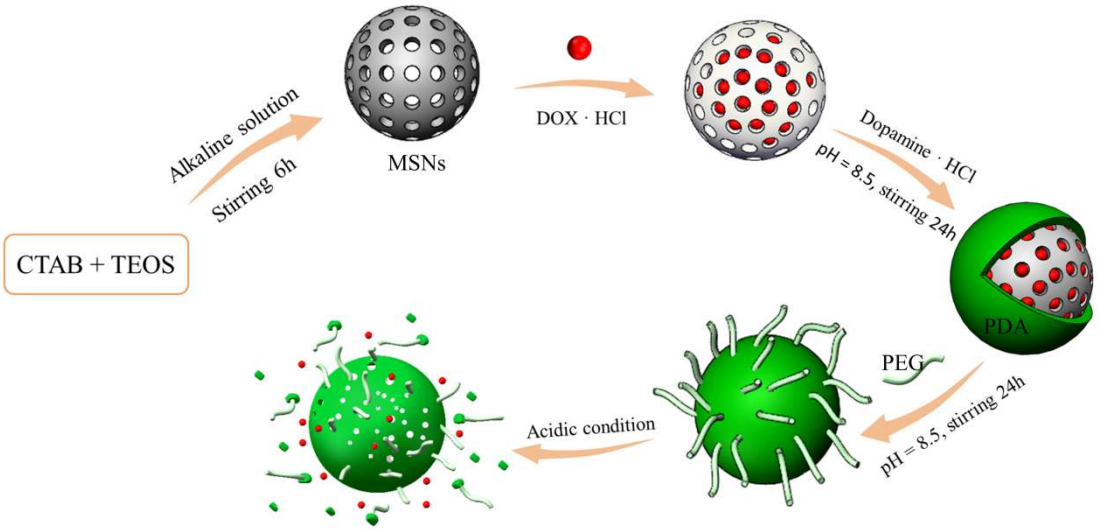
CTAB + TEOS
Alkaline solution
Stirring 6h
MSNs
DOX · HCl
Dopamine · HCl
pH = 8.5, stirring 24h
PDA
PEG
pH = 8.5, stirring 24h
Acidic condition

Scheme 1

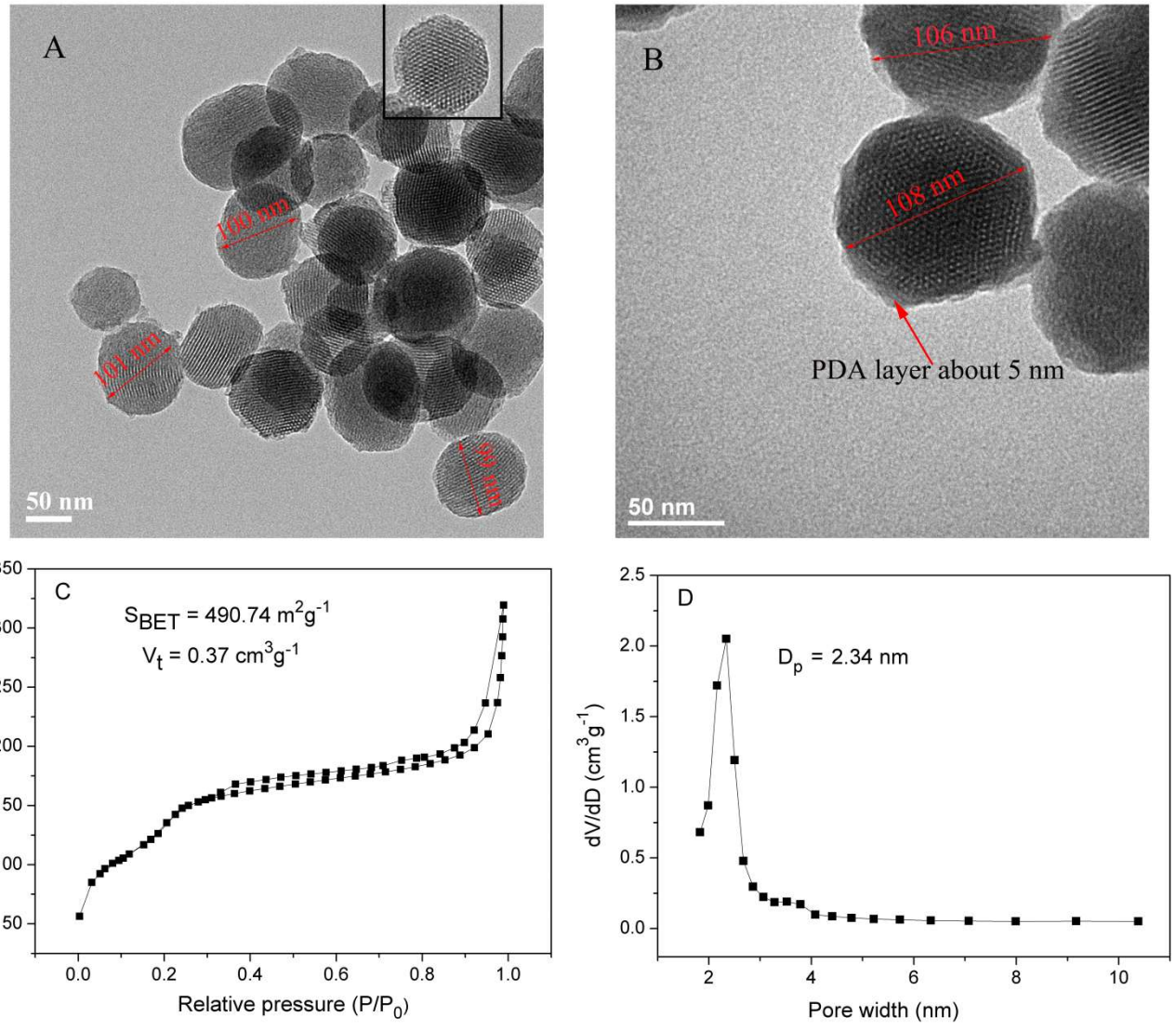
A
100 nm
103 nm
50 nm
50 nm
B
106 nm
108 nm
PDA layer about 5 nm
50 nm
C
S_{BET} = 490.74 m^2g^{-1}
V_t = 0.37 cm^3g^{-1}
Volume absorbed (cm^3g^{-1})
Relative pressure (P/P_0)
D
D_p = 2.34 nm
dV/dD (cm^3g^{-1})
Pore width (nm)

Fig. 1

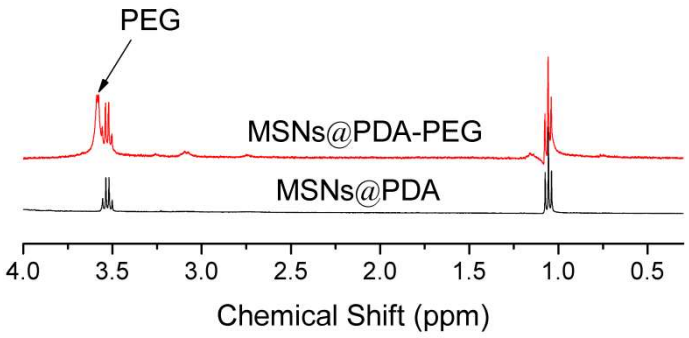

Fig. 2

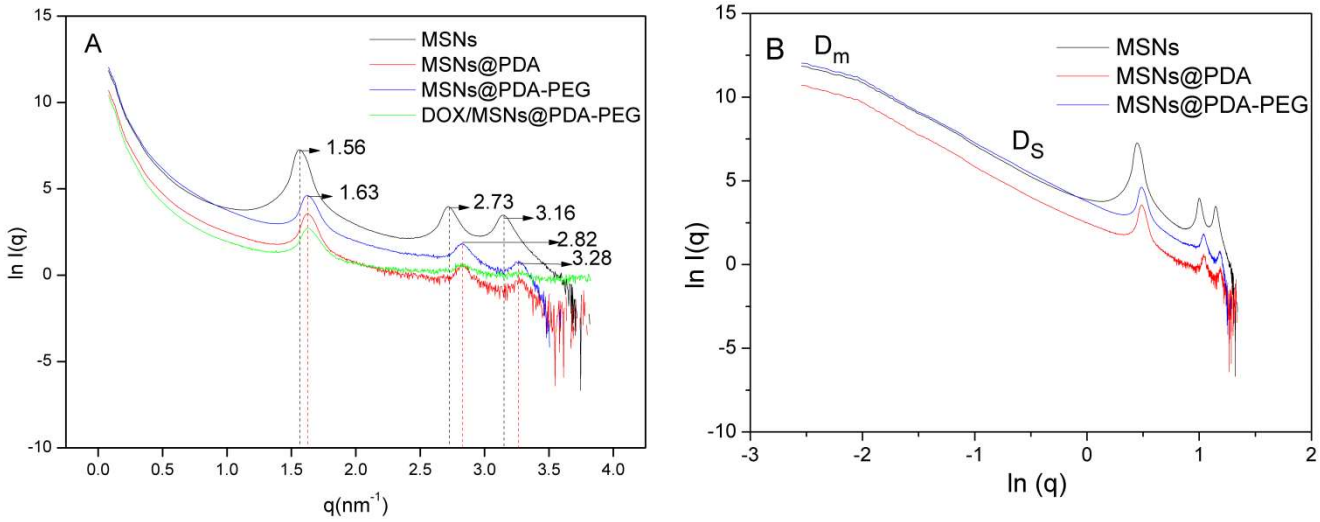

Fig. 3

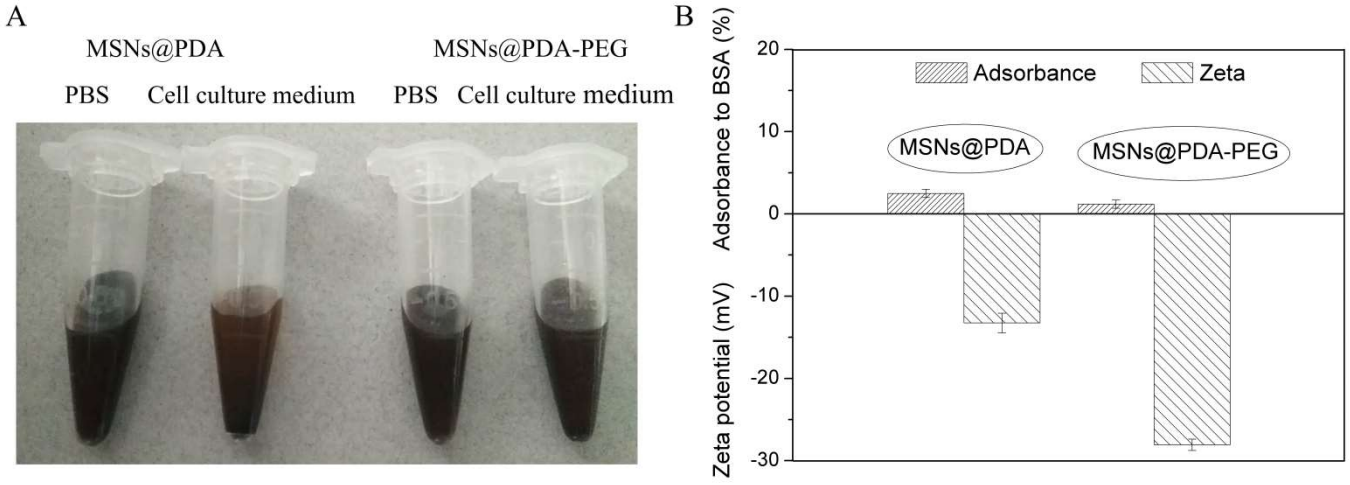

Fig. 4

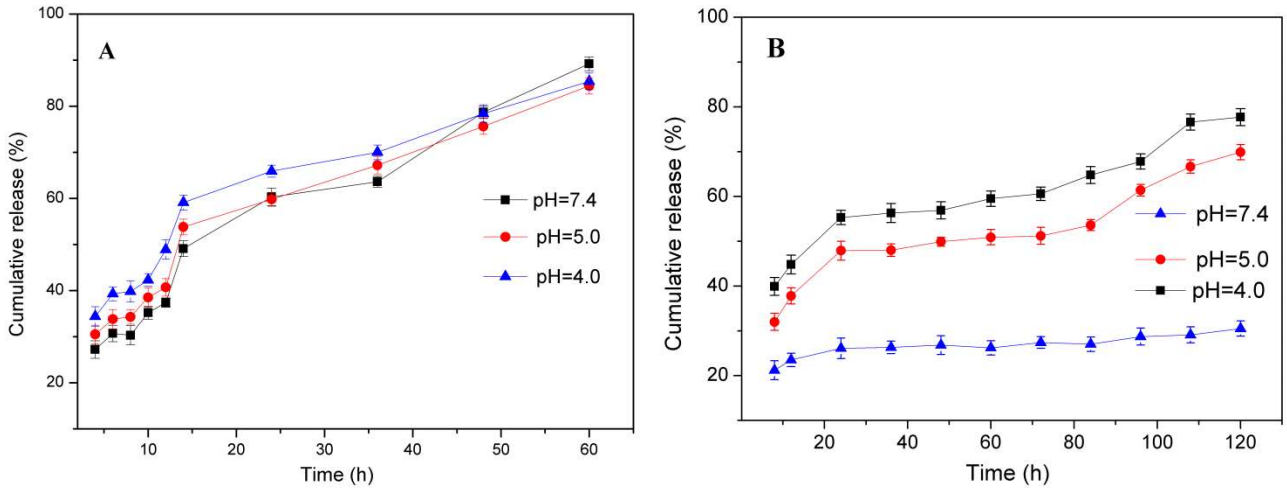

Fig. 5

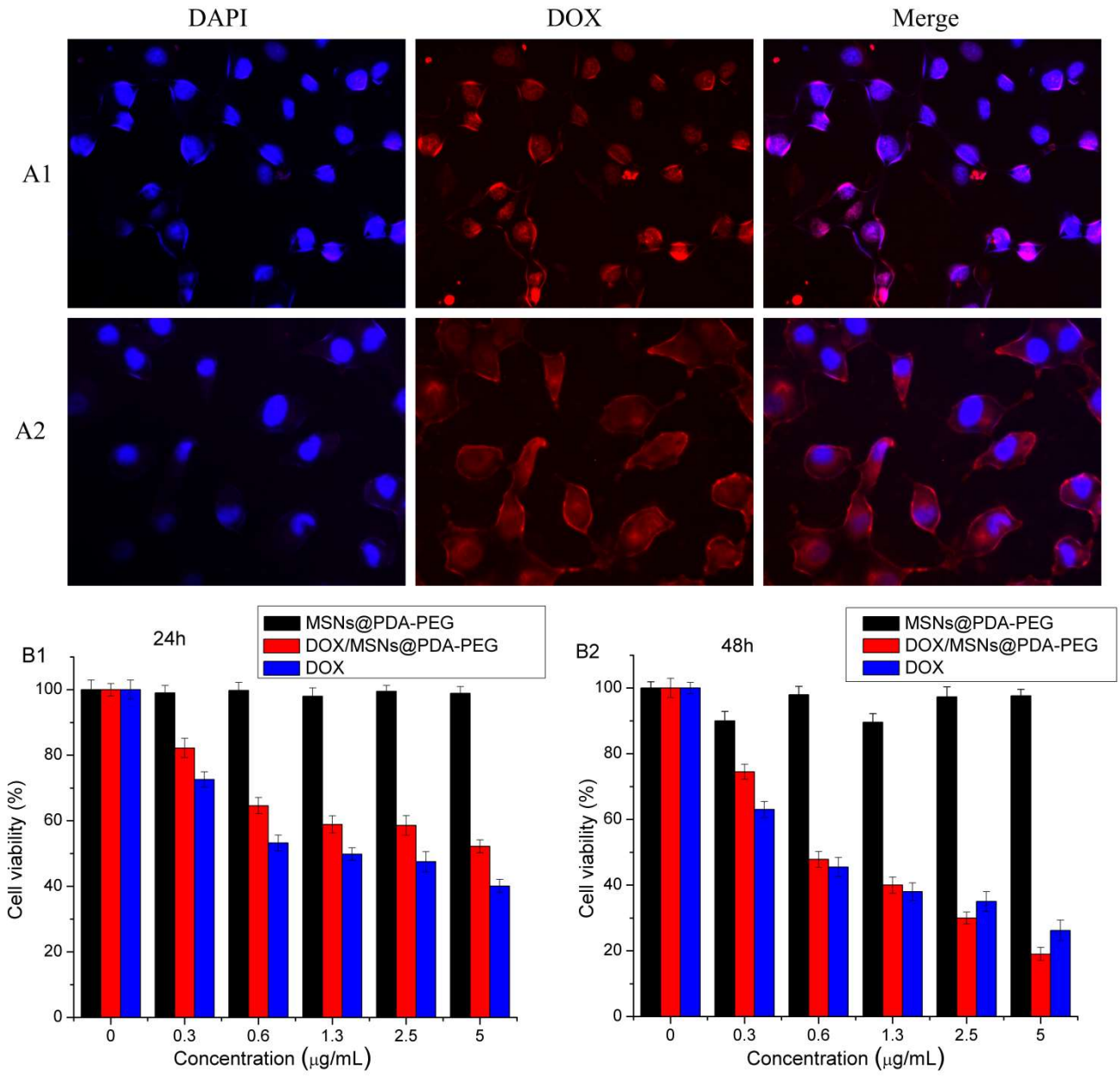

Fig. 6

Table 1 The fractal dimension variation of three samples determined from Fig. 4

Samples	D_m	D_s
MSNs	1.81 ± 0.05	3.76 ± 0.01
MSNs@PDA	1.77 ± 0.03	3.77 ± 0.01
MSNs@PDA-PEG	1.68 ± 0.02	3.69 ± 0.02

Note: all samples showed mass fractals (D_m) when $q < 0.14$ nm^{-1}, and showed surface fractals (D_s) when $q > 0.14$ nm^{-1}.